Spin Beats and Dynamical Magnetization in Quantum Structures

J. J. Baumberg and D. D. Awschalom
Department of Physics, University of California, Santa Barbara, California 93106

N. Samarth
Department of Physics, The Pennsylvania State University, University Park, Pennsylvania 16802

H. Luo and J. K. Furdyna
Department of Physics, University of Notre Dame, Notre Dame, Indiana 46556
(Received 7 October 1993)

A femtosecond-resolved Faraday spectroscopy has been developed to directly monitor spin dynamics in magnetically tunable semiconductor quantum wells. Tunable terahertz quantum beating of the optical polarization is observed from coherent excitation of the spin states Zeeman split by a single ultrathin magnetic tunneling barrier. Subsequent spin-flip scattering of photoinjected spin-polarized excitons deposits a magnetic "imprint" in the barrier which is orientation dependent and persists for orders of magnitude longer than the carrier lifetime.

PACS numbers: 73.20.Dx, 75.50.Rr, 78.20.Ls, 78.47.+p

The issue of spin dynamics within a matrix of interacting magnetic moments and charge carriers is an important problem in condensed matter physics. Recent advances in molecular beam epitaxy (MBE) of diluted magnetic semiconductors (DMS) enables simultaneous engineering of both band-gap energy and magnetic spin concentration in a single heterostructure, thereby producing "spin-engineered" environments for exploring such interactions [1,2]. By tailoring a specific geometry to confine electronic wave functions that penetrate a narrow magnetic tunneling barrier, one can witness *magnetic* behavior in low dimensions, which is otherwise difficult to observe. Here we investigate novel electronic and magnetic spin dynamics in magnetic-barrier-coupled double quantum wells (MCDQW) [3] using a femtosecond-resolved magneto-optical technique. Measurements reveal terahertz quantum beats between coherently excited carriers in Zeeman-split spin states through oscillations in the transmitted optical polarization. The period of this oscillatory Faraday rotation is tunable with applied magnetic field, and its amplitude is damped by ultrafast dephasing of the excited spin states. Moreover, spin-flip scattering takes several picoseconds longer and ceases before attaining carrier spin equilibrium. In contrast to traditional semiconductors, a long-lived magnetic "imprint" appears and persists long after carriers have recombined. These studies demonstrate the need to monitor magnetic interactions to determine true equilibrium in this class of systems.

The samples are II-VI diluted magnetic semiconductors grown by MBE on (100) GaAs substrates with a 6000 Å buffer and a 2000 Å cap of ZnSe. They consist of two nonmagnetic 40-Å-wide $Zn_{0.77}Cd_{0.23}Se$ quantum wells separated by a magnetic $Zn_{0.76}Mn_{0.24}Se$ barrier of thickness $L_B = 12$, 24, or 32 Å. For transmission experiments, a region of the GaAs substrate is etched away using standard methods and the sample mounted, strain-free, in a magneto-optic cryostat capable of $T = 1.8$–300 K and $B = 0$–9 T. The photon energy is tuned to the vicinity of the lowest heavy-hole exciton, this symmetric state lying ~ 30 meV below the corresponding asymmetric state for the 12 Å sample, and average powers below 30 μW used to minimize sample heating. Separate experiments confirm that the nanometer-thick magnetic barriers evoke a rotation which reverses in concert with the applied field and possesses the expected Faraday resonance [4]. Absorption and photoluminescence establish the sample quality and characterize the static properties [3,5].

The infrared output of a mode-locked Ti:sapphire laser system is frequency doubled in a nonlinear optical crystal to generate tunable blue-green 100 fs pulses matching the band-gap energies of these quantum well samples. A synchronously triggered acousto-optic crystal reduces the duty cycle of the pulse train to 1.5 MHz, allowing the complete recovery of long-lived magnetic signals. The selected pulses are divided into separately time delayed and mechanically chopped pump and probe beams that intersect at a 100 μm sample spot. Arcsecond Faraday rotations of the transmitted linearly polarized probe beam are resolved in an "optical bridge," which separates the orthogonal polarization components ($\pm 45°$) onto a pair of balanced photodiodes and detects small deviations from the null condition [4]. Pump-induced changes in the probe rotation are measured as a function of time delay between the pulses. Simultaneously, changes in probe transmission reveal the electronic carrier lifetime. A coherent artifact between pump and probe pulses confirms the position of zero delay to ± 50 fs and allows a 300 fs estimate of the system temporal response [5].

Figure 1 shows the initial few picoseconds of the time-resolved Faraday rotation from a 32 Å MCDQW sample at $T = 4.5$ K and clearly resolves oscillations in the emerging probe polarization. This change in Faraday rota-

0031-9007/94/72(5)/717(4)$06.00

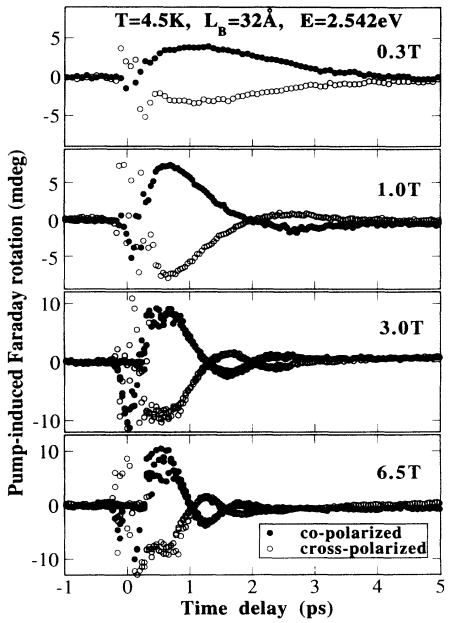

FIG. 1. Time-resolved Faraday rotation as a function of applied field probed by collinear (●) and crossed (○) polarizations of pump and probe pulses.

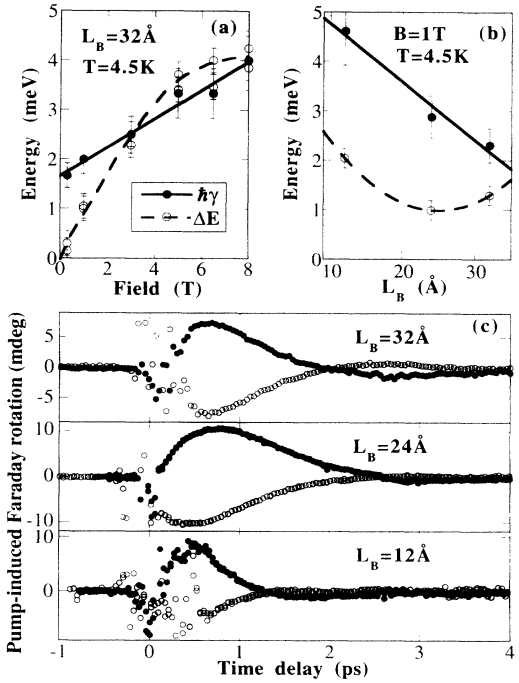

FIG. 2. (a) The separation, ΔE, and dephasing, $\hbar\gamma$, of the beating states in Fig. 1, calculated from their oscillation period and decay via $e^{-t/\tau_d}\sin(\Delta E\, t/\hbar)$. (b) Corresponding parameters as a function of barrier width, L_B. (c) Pump-induced Faraday rotation from collinear (●) and crossed (○) pump-probe linear polarizations in samples with three magnetic barrier widths under identical excitation conditions at $B=1$ T, $T=4.5$ K.

tion, which reflects the pump-induced circular birefringence of the heterostructure, demonstrates the existence of quantum beating of the index dispersions corresponding to spin-up ($|\uparrow\rangle$, $S_z=+1$) and spin-down ($|\downarrow\rangle$, $S_z=-1$) excitons. The beating originates from coherent excitation of a linear superposition of the coupled-quantum-well spin states ($\psi_0=|\uparrow\rangle+|\downarrow\rangle$) Zeeman split by the magnetic barrier. This is confirmed by orthogonally polarizing the pump and probe beams and observing a 180° phase shift introduced into the spin amplitudes ($\psi_0=|\uparrow\rangle-|\downarrow\rangle$). Because the excited carriers occupy a fraction of the available density of states, they reduce the oscillator strength of the transitions and perturb the corresponding refractive indices. Alternatively, the pump pulse sets the two spin states ringing at their respective frequencies and the reemitted nonlinear polarizations from these levels beat together in the optical bridge. The frequency of the oscillations is independent of the excitation density and probe power. The laser wavelength affects the oscillations' visibility, rather than their period, by changing the ratio of carrier densities excited into the two spin states. No oscillatory behavior or transient is observed in a control sample which substitutes a 12 Å nonmagnetic ZnSe tunneling barrier. Unlike conventional nonlinear optical schemes [6–8], these quantum beats are seen in a *single* double quantum well, therein alleviating concerns over sample inhomogeneity and interlayer magnetic coupling.

The oscillation frequency displayed in Fig. 2(a) measures the energy splitting between the spin states whose field dependence follows the Brillouin function characteristic of a system of paramagnetic spins. The splitting and saturation field compare well to static measurements on this sample [3]. The damping of these oscillations (Fig. 1) reflects the destruction of phase coherence between the excited levels, and is shown as a FWHM linewidth, $\hbar\gamma$, converted from the measured dephasing time, $\tau_d=2/\gamma$ [5]. For comparison the FWHM absorption linewidth of the heavy-hole exciton is ~20 meV independent of both magnetic field and barrier width. This implies that, although the energy of the lowest exciton level varies across the sample, the energy dispersion of the splitting between the spin states is at least an order of magnitude smaller. This latter inhomogeneous energy difference and the corresponding homogeneous linewidth, given by the total phase-scattering rate, both contribute to the measured dephasing. This dephasing rate, exclusively phase scattering at $B=0$, doubles as the applied field is increased to 8 T, in sharp contrast to the spin-scattering rates seen later. Inhomogeneities in the energy splitting seem slight as they would be expected to saturate with the magnetization. Figures 2(b) and 2(c) show data for a selection of tunneling barrier widths at $B=1$ T and $T=4.5$ K, where all of the samples are well below the magnetization saturation. The dephasing rate increases for thinner barriers while the magnetization seen in the spin splitting is smallest in the 24 Å sample. If a

major contribution to the decoherence is ascribed to interface and alloy disorder scattering in the magnetic barrier, then the phase scattering would be expected to follow the tunneling rate of carriers (increasing for narrow barriers). Furthermore, as a magnetic field is applied, both the tunneling rate for the favored spin-down carriers and potential fluctuations from the random distribution of Mn^{2+}, increase. These trends are different for the magnetization, possibly due to the effects of reduced dimensionality on the antiferromagnetic Mn^{2+} interaction [3]. Near the interfaces, these ions are subject to fewer nearest-neighbor forces and the effective magnetic concentration (normally depressed due to locking of the spins in clusters) may rise.

In order to focus on electronic spin scattering and dynamic magnetization, we use a circularly polarized pump pulse of appropriate helicity to excite carriers of specific spin orientation. Figure 3 shows the induced Faraday rotation at $B=0$ T which displays identical signals, apart from a sign change, with either orientation since the states are degenerate. Filling a state of one particular spin reduces its oscillator strength by Pauli exclusion and produces a circular birefringence of the corresponding sign. The rise time of the signal is pulse limited, and the decay contains two contributions of very different relaxation rate (Fig. 3, inset). The slower ~ 60 ps decay rate coincides with the carrier lifetime as measured simultaneously by induced transmission, and separately performed time-resolved photoluminescence (also shown) [9]. The fast ~ 4 ps transient corresponds to spin-scattering which

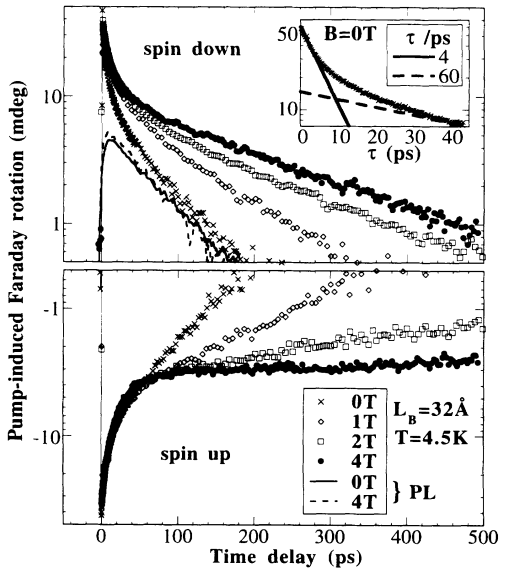

FIG. 3. Induced Faraday rotation at the spectral peak ($E=2.542$ eV) for $B=0$, 1, 2, 4 T when exciting spin-up or spin-down excitons using circular pump polarizations. Lines show the time-resolved photoluminescence at $B=0$ T (solid) and 4 T (dashed) for spin-down excitons. Inset: The two decay components at $B=0$ T.

transfers excitons from the initially excited spin population to the other vacant spin state, thus acting to restore equal oscillator strengths and reduce the Faraday rotation. The spin-scattering rate is unaffected by temperatures up to 30 K, but is 80% faster at energies a few meV above the peak exciton absorption. Against expectations, the scattering terminates after only 10 ps and the populations remain decoupled as they recombine instead of this entropically driven process continuing until spin densities equalize. Previous authors have associated two-component decays in induced transmission with separate electron and hole spin-flip rates [10], or the existence of optically inactive $J=2$ excitons [11]. However, such interpretations in this case would imply that either electron or hole spin scattering processes are far slower than the recombination rate. The nonequilibrium spin relaxation is not strongly correlated with temperature, pump intensity, or barrier width and although seen in related time-resolved photoluminescence measurements on similar samples [9], its origin remains unclear. As soon as magnetic fields $B>1$ T are applied to these structures, the spin-scattering rate decreases by 40%, suggesting that lifting the degeneracy reduces available final states. Therefore we find that magnetic fields repress spin-flip transitions but enhance scattering within each spin level.

In the presence of applied field, both time-resolved absorption and photoluminescence data confirm that the carrier lifetime is not significantly affected. However, Fig. 3 shows a long-lived magnetic imprint which remains after the carriers have recombined and persists for several nanoseconds. Unlike traditional semiconductor structures, the presence of magnetic spins introduces another relaxation process which redefines the time scale for equilibrium. This demonstrates the utility of time-resolved Faraday rotation as most optical techniques rely on carriers that no longer contribute information once they recombine. Injecting spin-up or spin-down carriers evokes different magnetic behavior, making it hard to associate the signals with purely thermal effects. Persistent signals from the pump-induced perturbation of the magnetization are found in all the MCDQW samples but not in the nonmagnetic control. Figure 3 shows that when spin-down excitons interact with the Mn^{2+} ions in an applied field, the magnetic decay remains exponential but becomes progressively slower. In the same field, when spin-up excitons are injected, this time scale rapidly stretches beyond the maximum pulse delay available. Because the laser bandwidth bridges the absorption linewidths, these characteristics are not a strong function of the photon energy. Such observations, in addition to spin-dependent scaling behavior of the signals with excitation density reported elsewhere [5], suggest a separate cause of the field-induced contributions in the two spin orientations.

Figure 4 presents further evidence in which the magnetic signature, calculated as the difference in pump-induced Faraday rotation between 4 and 0 T, is shown as

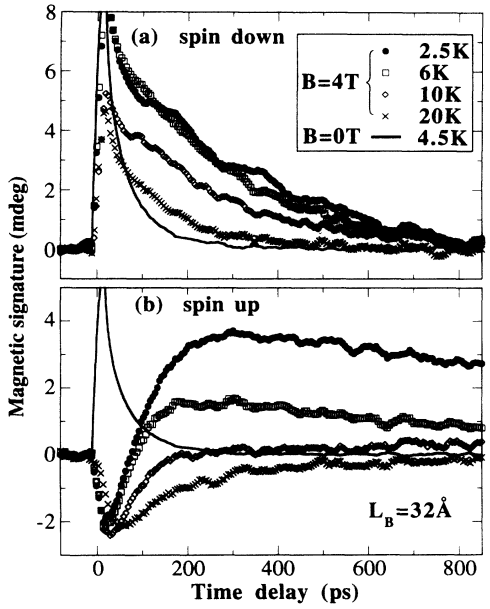

FIG. 4. Difference between time-resolved Faraday rotations at $B=0$ and 4 T (termed magnetic signature) for pumping (a) spin-down and (b) spin-up excitons as the temperature is increased. Zero-field signal shown for comparison (lines).

the lattice temperature is increased. Features appearing immediately after zero delay are dominated by changes in the overlap between the pump spectrum and field-shifted absorption lines of both spin states which lead to small differences in the carrier densities. Above $T=20$ K, the magnetic signatures for opposite spin orientations are similar. However, at lower temperatures where the static magnetization increases, an extra contribution appears in response to spin-up pumped excitons. The data confirm the expected selection rules for spin scattering which suggest that spin-down ($S_z=-5/2$) magnetic ions oriented by the applied field are scattered more efficiently by spin-up excitons than by spin-down excitons. As the injected excitons tunnel, they spin scatter, heating the effective spin temperature of the Mn^{2+} system above the lattice temperature. The magnetic ions then reorient on a much longer time scale (tens of nanoseconds) through spin-lattice relaxation processes.

In summary, femtosecond Faraday rotation allows the observation of both carrier spin and magnetic dynamics in quantum geometries. Magnetic tunneling barriers enhance exciton dephasing electronically and suppress spin scattering magnetically. Incorporating magnetic spins in conventional semiconductor heterostructures produces entirely different relaxation behavior and demonstrates a wealth of unexpected dynamical phenomena.

We thank S. Crooker and D. A. Tulchinsky for experimental contributions. This work was supported by Grants No. NSF DMR 92-07567, No. DMR 92-08400, and No. AFOSR F49620-93-1-0117, and by the IBM Corporation.

[1] N. Dai *et al.*, Phys. Rev. Lett. **67**, 3824 (1991); W. C. Chou *et al.*, Phys. Rev. Lett. **67**, 3820 (1991).
[2] D. D. Awschalom *et al.*, Phys. Rev. Lett. **66**, 1212 (1991); G. Bastard and L. L. Chang, Phys. Rev. B **41**, 7899 (1990).
[3] J. F. Smyth *et al.*, Phys. Rev. B **46**, 4340 (1992).
[4] J. J. Baumberg *et al.*, J. Appl. Phys. (to be published).
[5] J. J. Baumberg *et al.* (to be published).
[6] J. Shah, in *Optics of Semiconductor Nanostructures*, edited by F. Henneberger, S. Schmitt-Rink, and E. O. Göbel (Akademie Verlag, Berlin, 1993), pp. 149–180.
[7] K. Leo, in *Optics of Semiconductor Nanostructures* (Ref. [6]), pp. 127–148.
[8] S. Bar-Ad and I. Bar-Joseph, Phys. Rev. Lett. **66**, 2491 (1991).
[9] D. A. Tulchinsky *et al.* (to be published).
[10] S. Bar-Ad and I. Bar-Joseph, Phys. Rev. Lett. **68**, 349 (1992).
[11] M. Z. Maialle, E. A. de Silva, and L. J. Sham, Phys. Rev. B **47**, 15776 (1993).